4D.5 INVESTIGATING THE IMPACTS OF WAVE STATE AND SEA SPRAY ON TYPHOON VIA A COUPLED ATMOSPHERE-WAVE SYSTEM: THE IDEALIZED CASE

Bin Liu[1, 2]*, Changlong Guan[2], and Lian Xie[1]
[1]Department of Marine, Earth and Atmospheric Sciences, North Carolina State University, Raleigh, NC
[2]Physical Oceanography Laboratory, Ocean University of China, Qingdao, Shandong, China

1. INTRODUCTION

Air-sea momentum, heat and moisture fluxes are key processes in air-sea interaction, thus accurate calculation of these fluxes are essential to coupled air-sea modeling system. As a ubiquitous phenomenon at the sea surface, the existence of ocean surface waves modifies the boundary layer in both sides of the air and water interface, which in turn influence air-sea fluxes. Since early 90's, due to improved understanding of wave state effect on air-sea fluxes and the progress in high performance computing (HPC), extensive coupled atmosphere-wave studies have been conducted to investigate the impact of air-sea interactions on large-scale circulation (Weber et al., 1993; Janssen, 1994; Janssen and Viterbo, 1996; Weisse et al., 2000; Perrie and Zhang, 2001; Weisse and Schneggenburger, 2002), extratropical cyclones (Doyle, 1995; Lionello et al., 1998; Power and Stolinga, 2000; Desjardins et al., 2000; Lalbeharry et al., 2000) and tropical cyclones (Bao et al., 2000; Tenerelli et al., 2001; Doyle, 2002). Most previous studies utilized the wave-induced stress of Janssen (1989, 1991) or wave-age-dependent sea surface roughness (Smith et al., 1992; Donelan, 1993), in which younger waves correspond to rougher sea surface roughness, to parameterize air-sea momentum flux. However, based on recent field and laboratory observations, the SCOR workgroup 101 (Jones and Toba 2001) presented the SCOR relationship, showing that the nondimensional sea surface roughness first increases then decreases with the increasing wave age. Under high wind conditions, recent field and laboratory observations (Alamaro, 2001; Alamaro et al., 2002; Powell et al., 2003; Donelan et al., 2004) show that the drag coefficient does not increase, but decreases with the increasing wind because of sea foams and sea sprays.

The existence of sea sprays also has significant impacts on air-sea heat and moisture fluxes (e.g. Andreas, 1995). Many researchers investigated the effect of sea spray on air-sea interaction and atmospheric systems through including sea spray heat fluxes into atmospheric model or coupled air-sea system (Fairall et al., 1994; Kepert et al., 1999; Bao et al., 2000; Wang et al., 2001; Andreas and Emanuel, 2001; Li, 2004; Perrie et al., 2004; Zhang et al., 2006). However, these studies did not consider the effect of wave state on sea spray generation and sea spray heat flux, though it has been indicated that wave state has substantial impact on sea spray generation function (SSGF) and sea spray heat flux (Chaen, 1973;Iida et al., 1992; Piazzola et al., 2002; Zhao et al., 2006).

In addition, under high winds, dissipative heating can also have important effects on wind-wave coupled system. Previous studies (Bister and Emanuel, 1998; Zhang and Altshuler, 1999; Businger and Businger, 2001) have shown that taking into account dissipative heating increases tropical cyclone intensity by 10-20% as measured by the maximum surface wind. Thus, dissipative heating should also be included in the coupled atmosphere-wave model, particularly when concerning typhoon or hurricane systems.

Based on the parameterizations of air-sea momentum and heat fluxes including the effects of wave state and sea spray, the objective of the present study is to establish a coupled atmosphere-wave modeling system by using the Weather Research and Forecasting (WRF) model and the WAVEWATCH III (WW3) model. Several experiments are performed to simulate an idealized typhoon to investigate the impacts of sea-state-dependent roughness, dissipative heating and sea spray heat flux on typhoon systems.

2. THE COUPLED ATMOSPHERE-WAVE MODEL

The coupled atmosphere-wave modeling system consists of the WRF model and WW3 model. WRF V2.2 with the ARW dynamic core is used in this study. By incorporating the effects of wave state, sea spray and dissipative heating in wind-wave interactions, the WRF model is coupled to the WW3 model. Figure 1 illustrates the coupled atmosphere-wave modeling system, where the arrows demonstrate the directions of variable transfer between the model components. Details of the parameterization of the air-sea momentum and heat fluxes, the estimation of sea spray heat flux, as well as the dissipative heating are given in the following subsections.
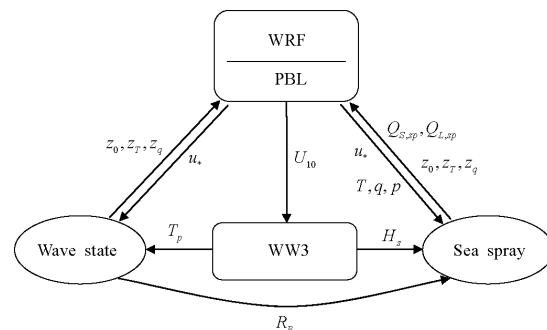

Figure 1. Schematic illustration of the coupled atmosphere-wave modeling system.

* Corresponding author address: Bin Liu, Department of Marine, Earth and Atmospheric Sciences, North Carolina State University, Raleigh, NC 27695; e-mail: bin_liu@ncsu.edu.

2.1 *The wave state and sea spray affected sea surface roughness*

In atmospheric models, air-sea momentum flux is usually estimated through the Charnock relation (Charnock, 1955)

$$g z_0 / u_*^2 = \alpha , \qquad (1)$$

where g is gravity, z_0 is the sea surface aerodynamic roughness, u_* is the friction velocity, and α is the Charnock constant which can also be thought of as the nondimensional roughness. In WRF the Charnock constant was chosen as 0.0185 following Wu (1980), which was widely used in other atmospheric and wave models. However, it has been gradually recognized that wave state has important influences on sea surface wind stress (Toba et al., 1990; Donelan et al., 1990; Johnson et al., 1998; Drennan et al., 2003), although there is a debate regarding in which way the wave state would influence the wind stress. Recently, the SCOR workgroup 101 (Jones and Toba 2001) presented the SCOR relation between the Charnock parameter and wave age, showing that the Charnock parameter first increases and then decreases with the increasing wave age, which, to some extent, can explain the existing field and laboratory observations. Since the SCOR relation is determined from observations mainly under wind speed less than 25 m s^{-1}, it is not suitable for applications under high wind conditions when sea foam and sea spray could have significant effects which led to a reduction of the drag coefficient and leveling off of surface wind stress (Alamaro, 2001; Alamaro et al., 2002; Powell et al., 2003; Donelan et al., 2004). Based on the solution of the TKE balance equation for the airflow in the regime of limited saturation by suspended sea spray droplets and field measurements of Powell et al. (2003), Makin (2005) derived a resistance law of the sea surface at hurricane winds, which can explain the reduction of the drag coefficient under high winds as a result of sea spray effects. However, this resistance law does not take into account the wave state effect.

In order to consider both wave state and sea spray effects on sea surface wind stress, by combining the SCOR relation and the resistance law of Makin (2005), Liu (2007) obtained a parameterization of sea surface aerodynamic roughness applicable to both low-to-moderate and high winds as:

$$\alpha = \begin{cases} (0.085\beta_*^{3/2})^{1-1/\omega} \left[0.03\beta_* \exp(-0.14\beta_*) \right]^{1/\omega}, & \beta_* < 35 \\ 17.60^{1-1/\omega} (0.008)^{1/\omega}, & \beta_* \geq 35 \end{cases}, \quad (2)$$

where $\beta_* = c_p / u_*$ is wave age, and $\omega = \min(1, \, a_{cr}/\kappa u_*)$ is correction parameter indicating the influence of sea spray on the logarithmic wind profile with κ the Karman constant, and the critical value of terminal fall velocity of the droplets a_{cr} =0.64 m s^{-1} (Makin, 2005). From equation (2) one can see that, under low-to-moderate winds when the sea spray effects can be neglected ($\omega = 1$) this parameterization is reduced into the SCOR relation; whereas, under high winds sea sprays have significant effects ($\omega < 1$), causing the reduction of the sea surface roughness and the drag coefficient. In this study, equation (2) is used to parameterize air-sea momentum flux in the coupled atmosphere-wave system in which both wave state and sea spray effects are included. In addition, the roughness under smooth surface due to molecular viscosity $z_s = 0.11\nu / u_*$, where ν is the kinematic molecular viscosity of air, is added to the sea surface roughness (Smith, 1988).

As for the sea surface heat and moisture fluxes, many field observations show that the air-sea exchange coefficients for sensible heat and water vapor are independent of wind speed, corresponding to the scalar roughnesses (z_T and z_q) decrease with the increasing wind speed. In the present study, the parameterization of sea surface scalar roughnesses from COARE algorithm V3.1 (Fairall et al., 2003):

$$z_T = z_q = \min\left(1.1\times10^{-4}, \; 5.5\times10^{-5} \, \mathrm{Re}_*^{-0.6}\right) \qquad (3)$$

where $\mathrm{Re}_* = z_0 u_* / \nu$ is the Reynolds number of sea surface aerodynamic roughness, is used to estimate the direct air-sea sensible and latent heat fluxes.

Since we are concerned about typhoon or hurricane system with extremely high wind and waves, other factors such as dissipative heating and sea sprays would also have significant impacts on air-sea heat and moisture fluxes.

2.2 *The dissipative heating*

The frictional dissipation of atmospheric kinetic energy finally occurs at molecular scales, which in turn is converted into thermal energy. Following Zhang and Altshuler (1999) the dissipative heating in the lowest level of the atmospheric model is expressed as

$$\left. \frac{dT}{dt} \right|_{Dis} = \frac{V_\mathbf{a} u_*^2}{C_p z_1} , \qquad (4)$$

where C_p is the air specific heat at constant pressure, z_1 is the height of model surface layer, and $V_\mathbf{a}$ is the wind speed at the model lowest semi-sigma layer. From equation (4) one can see that the dissipative heating is approximately proportional to the cubic power of surface wind speed. Thus under high winds, especially typhoon or hurricane conditions, dissipative heating increases rapidly with wind speed, which in turn will strengthen the typhoon or hurricane system. In the present coupled atmosphere-wave model, as we only consider the dissipative heating in the atmospheric surface layer (Bister and Emanuel, 1998; Zhang and Altshuler, 1999), it is equivalent to considering an upward sensible heat flux $H_E = \rho C_p V_a u_*^2$ at the bottom of the surface layer.

2.3 *The wave state affected sea spray heat flux*

Another important issue related to surface heat flux under high winds is the sea spray heat flux. In terms of the generation mechanism, there are mainly two kinds of spray droplets. One is bubble-derived droplets including film droplet and jet droplet produced by the

2

breaking of air bubbles when arising to sea surface within whitecaps. The radii of bubble-derived film and jet droplets are typically less than 5 and 20 μm, respectively. Another is spume droplet generated by wind tearing breaking wave crests, with its minimum radius generally about 20 μm (Andreas, 2002). To estimate the sea spray heat flux, one need to know the sea spray generation function (SSGF) dF/dr_0, which quantifies how many spray droplets of initial radius r_0 are produced per square meter of the surface per second per micrometer increment in droplet radius. The SSGF is usually considered as a function of wind speed and droplet radius (e.g. Monahan et al., 1986; Andreas, 1992; Wu, 1992; Smith et al., 1993; Fairall et al., 1994), while some studies found that the SSGF also depends on surface wave development (Chaen, 1973; Iida et al., 1992; Piazzola et al., 2002; Zhao et al., 2006). As to the SSGF for bubble-derived droplets, we introduce the whitecap coverage function of Zhao and Toba (2001)

$$W = 3.88 \times 10^{-5} R_B^{1.09} \qquad (5)$$

where $R_B = u_*^2 / \nu \omega_p$ is the windsea Reynolds number with ω_p the peak angular frequency of wave spectrum. Following Piazzola et al. (2002), substituting (5) into Monahan et al. (1986)'s SSGF, and using the relations between SSGF for different reference droplet radius (Andreas, 1992), we can obtain a windsea Reynolds number dependent SSGF:

$$\frac{dF}{dr_0} = 0.506 R_B^{1.09} r_0^{-2.95} \left(1 + 0.029 r_0^{1.02}\right) \times 10^{1.19\exp\left(-B_0^2\right)}$$
$$B_0 = \left(0.666 - 0.976 \log r_0\right)/0.650 \qquad (6)$$

As the windsea Reynolds number can also be expressed as $R_B = (g\nu)^{-1} u_*^3 \beta_*$, it can be thought of as a parameter simultaneously considering wind and wave state effects. From equation (6), we can see that with larger windsea Reynolds number associated with older waves, more spray droplets would be produced. Equation (6) is applicable to droplet radius between 0.8 to 20 μm (Andreas, 2002), since it is derived from Monahan et al. (1986)'s SSGF.

Connecting the SSGF applicable to bubble-derived droplets with Zhao et al. (2006)'s SSGF for spume droplets by filling the droplet radius gap between 20 and 30 μm through interpolation, one can thus obtain a wave state affected SSGF applicable to both bubble-derived droplet and spume droplet.

Considering the sea spray droplet microphysics (Andreas, 1989, 1990), Andreas (1992) estimated the "nominal" sea spray sensible and latent heat fluxes as

$$Q_s = \int_{r_{0,l}}^{r_{0,h}} Q_s(r_0) dr_0, \; Q_L = \int_{r_{0,l}}^{r_{0,h}} Q_L(r_0) dr_0, \qquad (7)$$

where $Q_s(r_0)$ and $Q_L(r_0)$ are sensible and latent heat fluxes contributed by droplets with initial radius r_0. Combining the feedback forms of Bao et al. (2002), Edson and Andreas (1997) and Andreas and DeCosmo (1999), we propose the following relation between the total sensible and latent heat fluxes, $H_{S,T}$ and $H_{L,T}$, and the nominal sea spray heat fluxes:

$$H_{S,T} = H_S + \beta Q_S - \alpha\gamma Q_L ,$$
$$H_{L,T} = H_L + \alpha Q_L \qquad (8)$$

where H_S and H_L are the direct air-sea sensible and latent heat fluxes without sea spray effect; and α, β, and γ are non-negative feedback coefficients indicating how the nominal sea spray heat fluxes contribute to the total sensible and latent heat fluxes. Thus, the net sea spray contribution to the total sensible and latent heat fluxes are

$$Q_{S,sp} = \beta Q_S - \alpha\gamma Q_L ,$$
$$Q_{L,sp} = \alpha Q_L \qquad (9)$$

which are called sea spray sensible and latent heat fluxes hereinafter. In this study, α and γ are determined following Bao et al. (2000), while β is taken as 1 (Andreas, 1992).

By using the new proposed SSGF and Andreas (1992)'s algorithm, and considering the feedback effects equation (8), we can now estimate the sea spray sensible and latent heat fluxes that include wave state effect. This method is used in the coupled atmosphere-wave modeling system to investigate the impacts of sea spray heat flux on typhoon systems.

3. THE IDEALIZED TYPHOON AND EXPERIMENT DESIGN

The idealized typhoon case set up in this study is based on the intensifying period, from 0000 UTC 31 August to 0000 UTC 3 September, of Typhoon Nabi over the North-Western Pacific Ocean in 2005. The model domain is centered at ($142°E$, $18°N$) with Lambert-conformal projection and 18 km grid spacing. The whole model area is assumed to be over ocean with 1000 m water depth. Sea surface temperature is set to 30 ℃ and kept constant during the model integration. The coupled system exchanges information between WRF and WW3 every 15 minutes. And the coupled system integrates 72 h forward from 0000 UTC 31 August, with the modeling results output at 3 h interval.

The WRF model contains 191×155 horizontal grid points, and 30 full-sigma layers in vertical direction, and the time step is 60 s. WSM5 microphysics scheme (Hong et al., 2004), Kain-Fritsch cumulus scheme (Kain and Fritsch, 1990, 1993), YSU PBL scheme, and Dudhia short wave (Dudhia, 1989) and RRTM long wave (Mlawer et al., 1997) radiation scheme are chosen in this case. The lateral conditions come from NCEP GFS $1° \times 1°$ reanalysis data. And the atmospheric model is initialized by a 12 h uncoupled WRF simulation (from 1200 UTC 30 August to 0000 UTC 31 August) with bogus vortex implanted at 1200 UTC 30 August based on the typhoon intensity and location data from JTWC.

The WW3 wave model resolves 32 frequencies logarithmically spaced from 0.041 to 0.790 Hz and 24 direction bands of 15 degrees each. The model grid points correspond to the mass grid points of the WRF model, and the time step is 15 minutes. Also the initial field is provided by the uncoupled 12 h WW3 simulation

(from 1200 UTC 30 August to 0000 UTC 31 August) driven by the wind from the uncoupled WRF simulation.

Four experiments are designed to evaluate the effects of wave state, sea spray and dissipative heating on typhoon system. Table 1 gives the summary of the experiments. CTRL is the control run with WRF and WW3 being uncoupled. The classical Charnock relation is used to parameterize the air-sea momentum flux, but dissipative heating and sea spray heat flux are not considered. Unlike the control run, CPLZ0 couples WRF to WW3 through the proposed wave state and sea spray affected surface roughness. CPLZ0DH considered both wave state and sea spray affected surface roughness and atmospheric surface layer dissipative heating. CPLFULL takes into account the effects of the wave state, sea spray and dissipative heating on air-sea momentum and heat fluxes, thus is the fully coupled experiment.

Table 1. The summary of the experiments.

Expt.	Aerodynamic roughness	Dissipative heating	Sea spray heat flux
CTRL	Equation (1)	No	No
CPLZ0	Equation (2)	No	No
CPLZ0DH	Equation (2)	Yes	No
CPLFULL	Equation (2)	Yes	Yes

Table 2. The simulated minimum SLP, maximum 10-m wind, and maximum SWH of the idealized typhoon for each experiment.

Expt.	Min SLP (hPa)	Max U_{10} (m s^{-1})	Max H_s (m)
CTRL	934.1	44.5	21.9
CPLZ0	938.1	45.6	20.5
CPLZ0DH	931.0	50.2	23.8
CPLFULL	923.4	52.5	22.7

4. EXPERIMENT RESULTS

4.1 *The influence of wave state and sea spray affected roughness*

Figure 2a-c show the simulated time series of the minimum sea level pressure (SLP), the maximum 10-m wind speed, and the maximum significant wave height (SWH) for each experiment. Table 2 lists the simulated minimum SLP, maximum 10-m wind, and maximum SWH of the idealized typhoon for each experiment. Comparing the CPLZ0 simulated minimum SLP to that of the control run, the typhoon intensity is weakened by the wave state effects due to increasing the sea surface roughness and surface friction. This is consistent with previous coupled atmosphere-wave studies (Doyle, 1995; Lionello et al., 1998; Tenerelli et al., 2001). The minimum central pressure (938.1 hPa) of CPLZ0 is 4 hPa higher than that of CTRL. However, the maximum 10-m wind speed is 45.6 m s^{-1}, which is increased by 2% relative to the control run due to the sea spray effect of reducing the drag coefficient and leveling off the wind stress in high wind areas. Although the maximum 10-m wind speed of CPLZ0 is a little larger than that of CTRL, the area with high wind speed (e.g. larger than 20 m s^{-1})

for the CPLZ0 run is smaller than that for the control run. As a result, the CPLZ0 simulated SWH is smaller than CTRL, with the maximum SWH being reduced by 1.4 m.
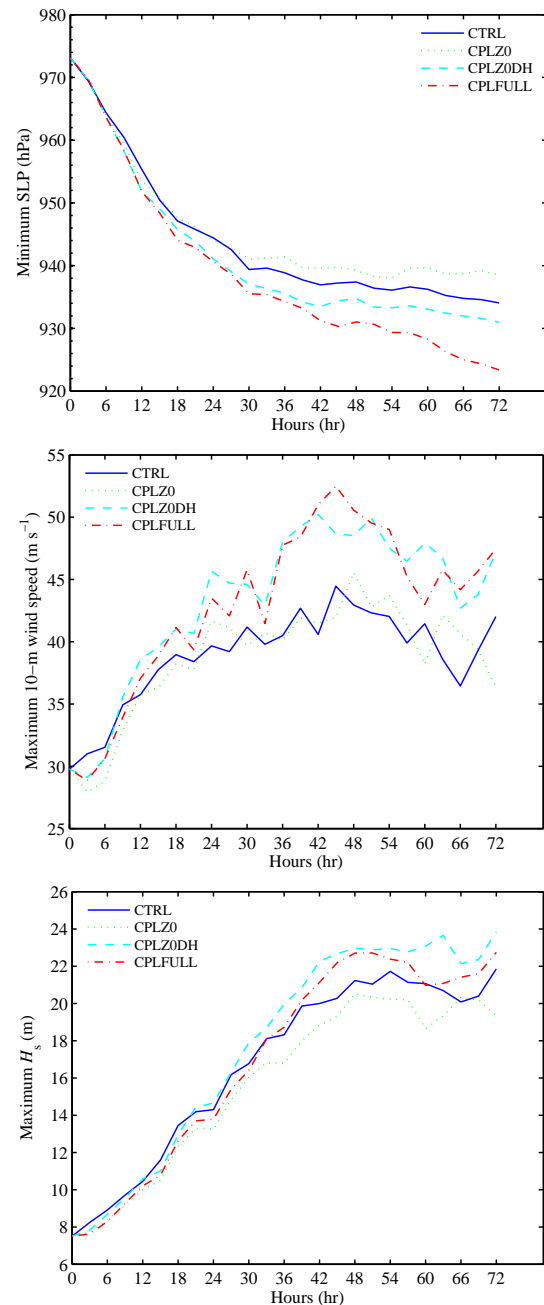

Figure 2. Time series of the simulated minimum sea level pressure (a), maximum 10-m wind speed (b) and maximum significant wave height (c) for each experiment.

Figure 4 gives the CPLZ0 simulated 48-h friction velocity (a), sea surface aerodynamic roughness (b), 10-m wind speed (c), wave age β_* (d), relation between the drag coefficient and 10-m wind speed (e), and relationship between the Charnock parameter and wave

4

age β_* (f). Experiment CPLZ0 considers the wave state and sea spray affected sea surface roughness, leading to the increase of surface roughness due to wave age effect under low to moderate winds but the decrease of surface roughness due to sea spray effect under high winds. The maximum sea surface roughness is located at the south section of the typhoon where the wind speed is not extremely high and the wave age is relatively small. From the CPLZ0 simulated relation between the drag coefficient and wind speed (Figure 4e), the drag coefficient is no longer linearly dependent upon wind speed because of wave age effects. The impact of sea spray reduces the drag coefficient under high wind conditions. Figure 4f illustrates the CPLZ0 simulated relation between the Charnock parameter and wave age, where the blue points correspond to wind speed less than 25 m s^{-1} and red circles correspond to wind speed larger than 25 m s^{-1}. It is shown that sea surface roughness decreases with wave age when wave age β_* is larger than about 6, and the existence of sea spray under high winds significantly reduces the sea surface roughness.

Table 3 lists the simulated 48-h total sensible heat flux $H_{S,T}$, total latent heat flux $H_{L,T}$, direct sensible heat flux H_S, direct latent heat flux H_L, equivalent sensible heat flux to dissipative heating H_E, sea spray sensible heat flux $Q_{S,sp}$, and sea spray latent heat flux $Q_{L,sp}$ for the 720×720 km^2 area centered at the typhoon eye for each experiment. There is no significant difference between the CTRL and CPLZ0 simulated sensible and latent heat fluxes, indicating that the impact of wave state and sea spray affected sea surface roughness on air-sea heat flux is negligible.

Table 3. Each experiment simulated 48-h $H_{S,T}$, $H_{L,T}$, H_S, H_L, H_E, $Q_{S,sp}$, and $Q_{L,sp}$ for the 720x720 km^2 area centered at the typhoon eye. The unit is 10^4 W m^{-2}.

Expt.	$H_{S,T}$	$H_{L,T}$	H_S	H_L	H_E	$Q_{S,sp}$	$Q_{L,sp}$
CTRL	8.78	98.86	8.78	98.86	-	-	-
CPLZ0	8.45	99.48	8.45	99.48	-	-	-
CPLZ0DH	19.16	105.60	5.03	105.60	14.13	-	-
CPLFULL	1.49	116.99	12.77	82.08	11.73	-23.00	34.92

4.2 *The influence of dissipative heating*

From Figure 2 and Table 2, one can see that, comparing the results of CPLZ0DH to those of CPLZ0, the CPLZ0DH simulated minimum central pressure is 7.9 hPa deeper than the CPLZ0 run, and the maximum 10-m wind speed and the maximum SWH are also increased by 10% and 16%, respectively. These results are in agreement with previous studies (Bister and Emanuel, 1998; Zhang and Altshuler, 1999). While comparing experiment CPLZ0DH to the control run, taking into account both wave state and sea spray effected sea surface roughness and dissipative heating makes the minimum central pressure 3.1 hPa deeper

than the CTRL run, and a 13% increase of the maximum wind speed as well as a 9% increase of the maximum SWH.
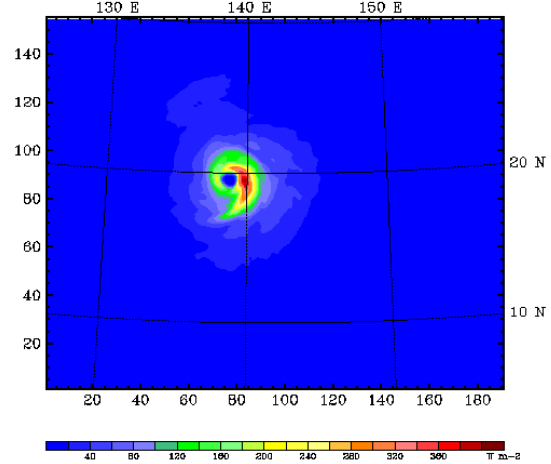

Figure 3. The simulated 48-h equivalent sensible heat flux to dissipative heating H_E for CPLZ0DH.

Figure 3 shows the CPLZ0DH simulated 48-h equivalent sensible heat flux to dissipative heating H_E. Due to the cubic power dependence on wind speed, the dissipative heating is significant in high wind areas, but very small in low wind areas. From Table 3 which lists the heat fluxes for the selected area, relative to the control run CPLZ0DH simulated total sensible and latent heat flux increased by 120% and 6%, respectively, leading to a 16% increase in the total heat flux.

4.3 *The influence of sea spray heat flux*

In Figure 2 and Table 2, the fully coupled experiment CPLFULL obtains the lowest minimum SLP (923.4 hPa), which is 14.7 hPa deeper than CPLZ0 and 10.7 hPa deeper than the control run. The CPLFULL simulated maximum 10-m wind speed is 52.5 m s^{-1}, 18% and 14% stronger than those of CPLZ0 and CTRL, respectively. The CPLFULL simulated maximum SWH is also increased by 11% and 4% relative to CPLZ0 and CTRL, respectively.

Figure 5 shows the CPLFULL simulated 48-h total sensible heat flux $H_{S,T}$ (a), total latent heat flux $H_{L,T}$ (b), direct sensible heat flux H_S (c), direct latent heat flux H_L (d), sea spray sensible heat flux $Q_{S,sp}$ (e), and sea spray latent heat flux $Q_{L,sp}$ (f). One can see that the sea spray sensible and latent heat fluxes are significant in areas with strong winds and waves. The sea spray sensible heat flux is negative, thus makes a negative contribution to the total upward sensible heat flux. Whereas, the sea spray latent heat flux makes a positive contribution to the total latent heat flux. Comparing with experiment CTRL and CPLZ0, sea spray heat flux increases the direct sensible heat flux but decreases the direct latent heat flux. This is because the evaporation of the spray droplets reduces low level air temperature and increases low level moisture, thus

increases air-sea temperature difference and reduces the air-sea moisture difference. From Table 3 where the heat fluxes for the 720×720 km^2 area centered at the typhoon center are listed, the fully coupled experiment CPLFULL simulated total heat flux is increased by 10% relative to the control run, with the latent heat flux increased by 18%.

5. CONCLUSIONS

In this study, a coupled atmosphere-wave modeling system, consists of the atmospheric WRF model and the WW3 wave model, was established based on the wave state and sea spray affected parameterization of air-sea momentum and heat fluxes as well as atmospheric dissipative heating. An idealized typhoon was selected and several simulations were performed by using the coupled modeling system to investigate the impacts of wave state and sea spray affected roughness, dissipative heating, and sea spray heat flux on a typhoon system.

Using the wave state and sea spray affected sea surface roughness instead of the classical Charnock relation led to a weakening of the typhoon system due to the increased surface roughness. The minimum central pressure increased by about 4 hPa and the maximum significant wave height is reduced by about 6%. While the maximum 10-m wind speed is increased by about 2% due to a decrease of drag coefficient at high wind speed caused by the sea spray effects. The inclusion of dissipative heating increases the air-sea heat flux and intensifies the typhoon system. Together with the wave state and sea spray affected surface roughness, atmospheric low level dissipative heating leads to a 13% increase of surface wind speed associated with 9% increase of the significant wave height relative to the control run. The air-sea heat flux was also increased by 16%. Taking into account the wave state affected sea spray heat flux also strengthens the typhoon system. It is noteworthy that the impacts of wave state and sea spray affected surface roughness, dissipative heating, and sea spray heat flux interact with each other through marine boundary layer processes. With all the three impacts included, the minimum central pressure simulated by the fully coupled experiment is 10.7 hPa deeper than the uncoupled run, with the maximum wind speed and significant wave height increasing by 14% and 4%, respectively. The total air-sea heat flux is also increased by 10%, with the latent heat flux increasing a more significantly 18%.

6. REFERENCES

Alamaro, M., 2001: Wind Wave Tank for Experimental Investigation of Momentum and Enthalpy Transfer from the Ocean Surface at High Wind Speed, Master thesis at Department of Earth, Atmospheric and Planetary Sciences, Massachusetts Institute of Technology, 79.

Alamaro, M., K. A. Emanuel, J. J. Colton, W. R. McGillis, and J. Edson, 2002: Experimental Investigation of Air-Sea Transfer of Momentum and Enthalpy at High Wind Speed. *25th Conference on Hurricanes and Tropical Meteorology*, San Diego, Ca., 2.

Andreas, E. L., 1989: Thermal and Size Evolution of Sea Spray Droplets. CRREL Rep. 89-11, 37 pp.

——, 1990: Time constants for the evolution of sea spray droplets. *Tellus, Ser. B*, **42,** 481-497.

——, 1992: Sea Spray and the Turbulent Air-Sea Heat Fluxes. *J. Geophys. Res.*, **97,** 11429-11441.

——, 2002: A review of the sea spray generation function for the open ocean. *Atmosphere-Ocean Interactions*, W. Perrie, Ed., WIT Press, 1-46.

Andreas, E. L. and J. DeCosmo, 1999: *Sea Spray Production and Influence on Air-Sea Heat and Moisture Fluxes over the Open Ocean. Air-Sea Exchange: Physics, Chemistry and Dynamics*, Kluwer Academic Publishers, 327-362 pp.

Andreas, E. L. and K. A. Emanuel, 2001: Effects of Sea Spray on Tropical Cyclone Intensity. *J. Atmos. Sci.*, **58,** 3741-3751.

Andreas, E. L., J. B. Edson, E. C. Monahan, M. P. Rouault, and S. D. Smith, 1995: The Spray Contribution to Net Evaporation from the Sea: A Review of Recent Progress. *Boundary-Layer Meteorol.*, **72,** 3-52.

Bao, J.-W., J. M. Wilczak, J.-K. Choi, and L. H. Kantha, 2000: Numerical simulations of air-sea interaction under high wind conditions using a coupled model: A study of hurricane development. *Mon. Wea. Rev.*, **128,** 2190-2210.

Bister, M. and K. A. Emanuel, 1998: Dissipative heating and hurricane intensity. *Meteor. Atmos. Phys.*, **65,** 233-240.

Businger, S. and J. A. Businger, 2001: Viscous Dissipation of Turbulence Kinetic Energy in Storms. *J. Atmos. Sci.*, **58,** 3793-3796.

Chaen, M., 1973: Studies on the production of sea-salt particles on the sea surface. *Mem. Fac. Fish., Kagoshima Univ.*, **22,** 49-107.

Charnock, H., 1955: Wind stress on a water surface. *Quart. J. Roy. Meteor. Soc.*, **81,** 639-640.

Desjardins, S., J. Mailhot, and R. Lalbeharry, 2000: Examination of the Impact of a Coupled Atmospheric and Ocean Wave System. Part I: Atmospheric Aspects. *J. Phys. Oceanogr.*, **30,** 385-401.

Donelan, M. A., 1990: Air-sea interaction. *The sea: Ocean Engineering Science*, B. l. Mehaute and D. M. Hanes, Eds., Wiley-Interscience, 239-292.

Donelan, M. A., F. W. Dobson, S. D. Smith, and R. J. Anderson, 1993: On the Dependence of Sea Surface Roughness on Wave Development. *J. Phys. Oceanogr.*, **23,** 2143-2149.

Donelan, M. A., B. K. Haus, N. Reul, W. J. Plant, M. Stiassnie, H. C. Graber, O. B. Brown, and E. S. Saltzman, 2004: On the limiting aerodynamic roughness of the ocean in very strong winds. *Geophys. Res. Lett.*, **31,** L18306, doi:10.1029/2004GL019460.

Doyle, J. D., 1995: Coupled ocean wave/atmosphere mesoscale model simulations of cyclogenesis. *Tellus*, **47A,** 766-788.

——, 2002: Coupled atmosphere-ocean wave simulations under high wind conditions. *Mon. Wea. Rev.*, **130,** 3087-3099.

Drennan, W. M., H. C. Graber, D. Hauser, and C. Quentin, 2003: On the wave age dependence of wind stress over pure wind seas. *J. Geophys. Res.*, **108,** 8062, doi:10.1029/2000JC000715.

Dudhia, J., 1989: Numerical study of convection observed during the winter monsoon experiment using a mesoscale two-dimensional model. *J. Atmos. Sci.*, **46,** 3077-3107.

Edson, J. B. and E. L. Andreas, 1997: Modeling the Role of Sea Spray on Air-SeaHeat andMoisture Exchange. *12th Symposium on Boundary Layers and Turbulence*, American Meteorological Society, Boston, MA, 490-491.

Fairall, C. W., J. D. Kepert, and G. J. Holland, 1994: The Effect of Sea Spray on Surface Energy Transports over the Ocean. *Global Atmos. Ocean Sys.*, **2,** 121-142.

Fairall, C. W., E. F. Bradley, J. E. Hare, A. A. Grachev, and J. B. Edson, 2003: Bulk Parameterization of Air-Sea Fluxes: Updates and Verification for the COARE Algorithm. *Journal of Climate*, **16,** 571-591.

Hong, S.-Y., J. Dudhia, and S.-H. Chen, 2004: A Revised Approach to Ice Microphysical Processes for the Bulk Parameterization of Clouds and Precipitation. *Mon. Wea. Rev.*, **132,** 103-120.

Iida, N., Y. Toba, and M. Chaen, 1992: A new expression for the production rate of sea water droplets on the sea surface. *J. Oceanogr.*, **48,** 439-460.

Janssen, P. A. E. M., 1989: Wave-induced stress and the drag of airflow over sea waves. *J. Phys. Oceanogr.*, **19,** 745-754.

——, 1991: Quasi-linear theory of wind-wave generation applied to wave forecasting. *J. Phys. Oceanogr.*, **21,** 1631-1642.

——, 1994: Results with a coupled wind wave model. ECMWF Tech. Rep. No. 71, 58 pp.

Janssen, P. A. E. M. and P. Viterbo, 1996: Ocean waves and the atmospheric climate. *Journal of Climate*, **9,** 1296-1287.

Johnson, H. K., J. Hojstrup, H. J. Vested, and S. E. Larsen, 1998: On the Dependence of Sea Surface Roughness on Wind Waves. *J. Phys. Oceanogr.*, **28,** 1702-1716.

Jones, I. S. F. and Y. Toba, 2001: *Wind stress over the ocean*. Cambridge University Press, 307 pp.

Kain, J. S. and J. M. Fritsch, 1990: A one-dimensional entraining/ detraining plume model and its application in convective parameterization. *J. Atmos. Sci.*, **47,** 2784-2802.

——, 1993: Convective parameterization for mesoscale models: The Kain-Fritcsh scheme. *The representation of cumulus convection in numerical models*, K. A. Emanuel and D. J. Raymond, Eds., Amer. Meteor. Soc., 246.

Kepert, J. D., C. W. Fairall, and J.-W. Bao, 1999: *Modelling the Interaction between the Atmospheric Boundary Layer and Evaporating Sea Spray Droplets. Air-Sea Exchange: Physics, Chemistry and Dynamics*, Kluwer Academic Publishers, 363-409 pp.

Lalbeharry, R., J. Mailhot, S. Desjardins, and L. Wilson, 2000: Examination of the impact of a coupled atmospheric and ocean wave system. Part II: Ocean wave aspects. *J. Phys. Oceanogr.*, **30,** 402-415.

Li, W., 2004: Modelling air-sea fluxes during a western Pacific typhoon: Role of sea spray. *Adv. Atmos. Sci.*, **21,** 269-276.

Lionello, P., P. Malguzzi, A. Buzzi, and, 1998: On the coupling between the atmospheric circulation and the ocean wave field: an idealized case. *J. Phys. Oceanogr.*, **28,** 161-177.

Liu, B., 2007: Physical basis and numerical study of the coupled atmosphere-wave model, Physical Oceanography Laboratory, Ocean University of China, 156.

Makin, V. K., 2005: A Note on the Drag of the Sea Surface at Hurricane Winds. *Boundary-Layer Meteorol.*, **115,** 169-176.

Mlawer, E. J., S. J. Taubman, P. D. Brown, M. J. Iacono, and S. A. Clough, 1997: Radiative transfer for inhomogeneous atmosphere: RRTM, a validated correlated-k model for the longwave. *J. Geophys. Res.*, **102,** 16663-16682.

Monahan, E. C., 1986: The ocean as a source for atmospheric particles. *The Role of Air-Sea Exchange in Geochemical Cycling*, P. Buat-Menard, Ed., D. Reidel, Dordrecht, 129-163.

Perrie, W. and Y. Zhang, 2001: A regional climate model coupled to ocean waves: Synoptic to multimonthly simulations. *J. Geophys. Res.*, **106,** 17753-17771.

Perrie, W., W. Zhang, X. Ren, Z. Long, E. L. Andreas, J. Gyakum, and R. McTaggart-Cowan, 2004: The role of waves, sea spray and the upper ocean in midlatitude storm development. *CD-ROM of preprints, 26th Conference on Hurricanes and Tropical Meteorology of the American Meteorological Society*, Miami, FL, 2.

Piazzola, J., P. Forget, and S. Despiau, 2002: A sea spray generation function for fetch-limited conditions. *Ann. Geophys.*, **20,** 121-131.

Powell, M. D., P. J. Vickery, and T. A. Reinhold, 2003: Reduced drag coefficient for high wind speeds in tropical cyclones. *Nature*, **422,** 279-283.

Powers, J. G. and M. T. Stoelinga, 2000: A coupled air-sea mesoscale model: Experiments in atmospheric sensitivity to marine roughness. *Mon. Wea. Rev.*, **128,** 208-228.

Smith, S. D., 1988: Coefficients for sea surface wind stress, heat flux, and wind profiles as a function of wind speed and temperature. *J. Geophys. Res.*, **93,** 15467-15472.

Smith, S. D., R. J. Anderson, W. A. Oost, C. Kraan, N. Maat, J. DeCosmo, K. B. Katsaros, K. L. Davidson, K. Bumke, L. Hasse, and H. M. Chadwick, 1992: Sea surface wind stress and drag coefficients: the HEXOS results. *Boundary-Layer Meteorol.*, **60,** 109-142.

Tenerelli, J. E., S. S. Chen, W. Zhao, and M. A. Donelan, 2001: High-resolution simulations of hurricane Floyd using MM5 coupled with a wave model. *Workshop Program for the Eleventh PSU/NCAR MM5 Users' Workshop*, 4.

Toba, Y., N. Iida, H. Kawamura, N. Ebuchi, and I. S. F. Jones, 1990: The wave dependence of sea-surface wind stress. *J. Phys. Oceanogr.*, **20,** 705-721.

Wang, Y., J. D. Kepert, and G. J. Holland, 2001: The Effect of Sea Spray Evaporation on Tropical Cyclone Boundary Layer Structure and Intensity. *Mon. Wea. Rev.*, **129,** 2481-2500.

Weber, S. L., H. v. Storch, P. Viterbo, and L. Zambresky, 1993: Coupling an ocean wave model to an atmospheric general circulation model. *Climate Dyn.*, **9,** 53-61.

Weisse, R. and C. Schneggenburger, 2002: The effect of different sea state dependent roughness parameterizations on the sensitivity of the atmospheric circulation in a regional model. *Mon. Wea. Rev.*, **130,** 1595-1602.

Weisse, R., H. Heyen, and H. V. Storch, 2000: Sensitivity of a regional atmospheric model to a sea state-dependent roughness and the need for ensemble calculations. *Mon. Wea. Rev.*, **128,** 3631-3642.

Wu, J., 1980: Wind-stress coefficients over sea surface near neutral conditions - A revisit. *J. Phys. Oceanogr.*, **13,** 1441-1451.

——, 1992: Bubble flux and marine aerosol spectra under various wind velocities. *J. Geophys. Res.*, **97,** 2327-2333.

Zhang, D.-L. and E. Altshuler, 1999: The Effects of Dissipative Heating on Hurricane Intensity. *Mon. Wea. Rev.*, **127,** 3032-3038.

Zhang, W., W. Perrie, and W. Li, 2006: Impacts of Waves and Sea Spray on Midlatitude Storm Structure and Intensity. *Mon. Wea. Rev.*, **134,** 2418-2442.

Zhao, D. and Y. Toba, 2001: Dependence of whitecap coverage on wind and wind-wave properties. *J. Oceanogr.*, **57,** 603-616.

Zhao, D., Y. Toba, K.-i. Sugioka, and S. Komori, 2006: New sea spray generation function for spume droplets. *J. Geophys. Res.*, **111,** C02007, doi:10.1029/2005JC002960.
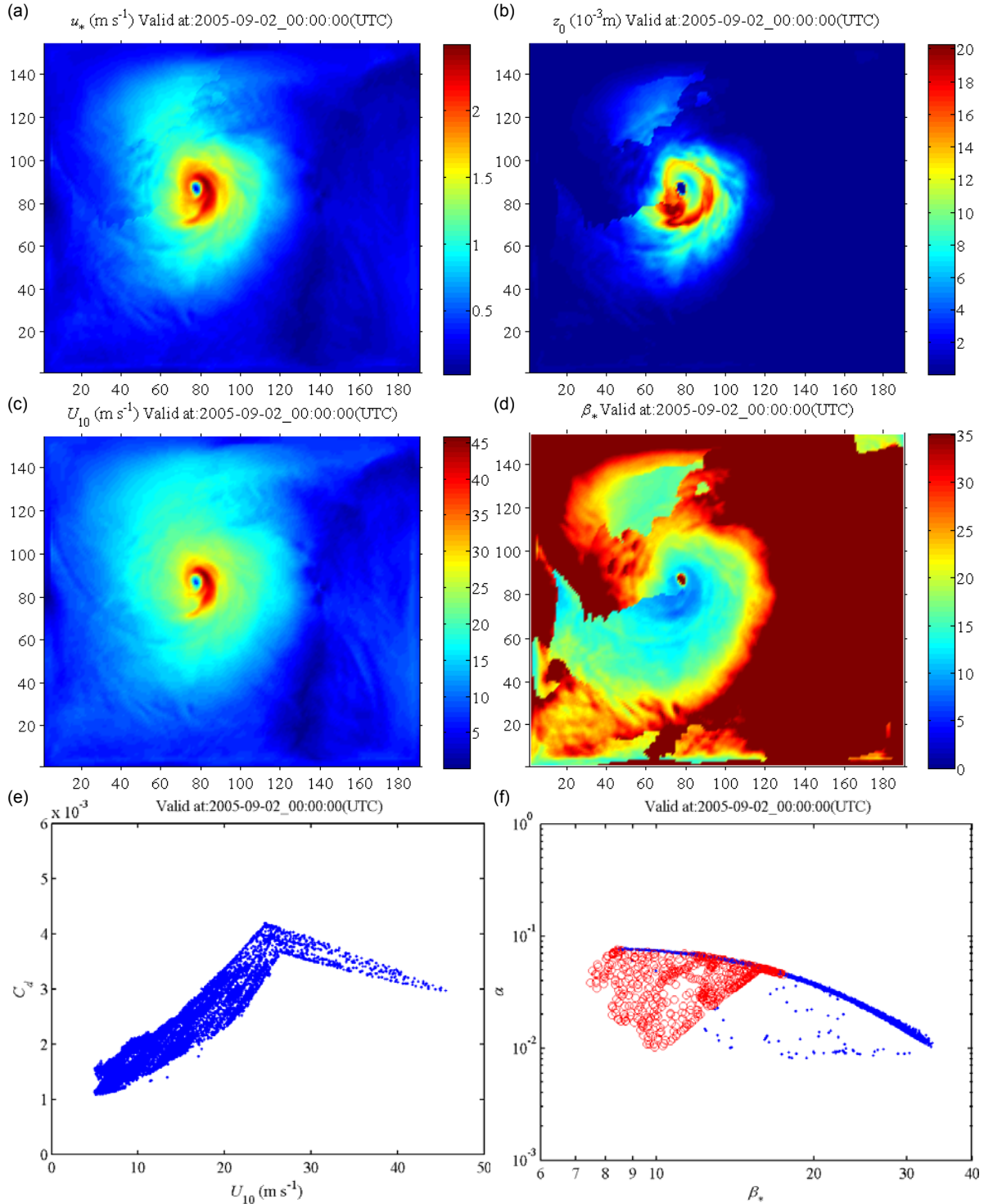
Figure 4. The simulated 48-h friction velocity (a), sea surface aerodynamic roughness (b), 10-m wind speed (c), wave age β_* (d), relation between the drag coefficient and 10-m wind speed (e), and relationship between the Charnock parameter and wave age β_* for experiment CPLZ0. The blue points in (f) correspond to 10-m wind speed less than 25 m s^{-1}, while the red circles correspond to 10-m wind speed larger than 25 m s^{-1}.
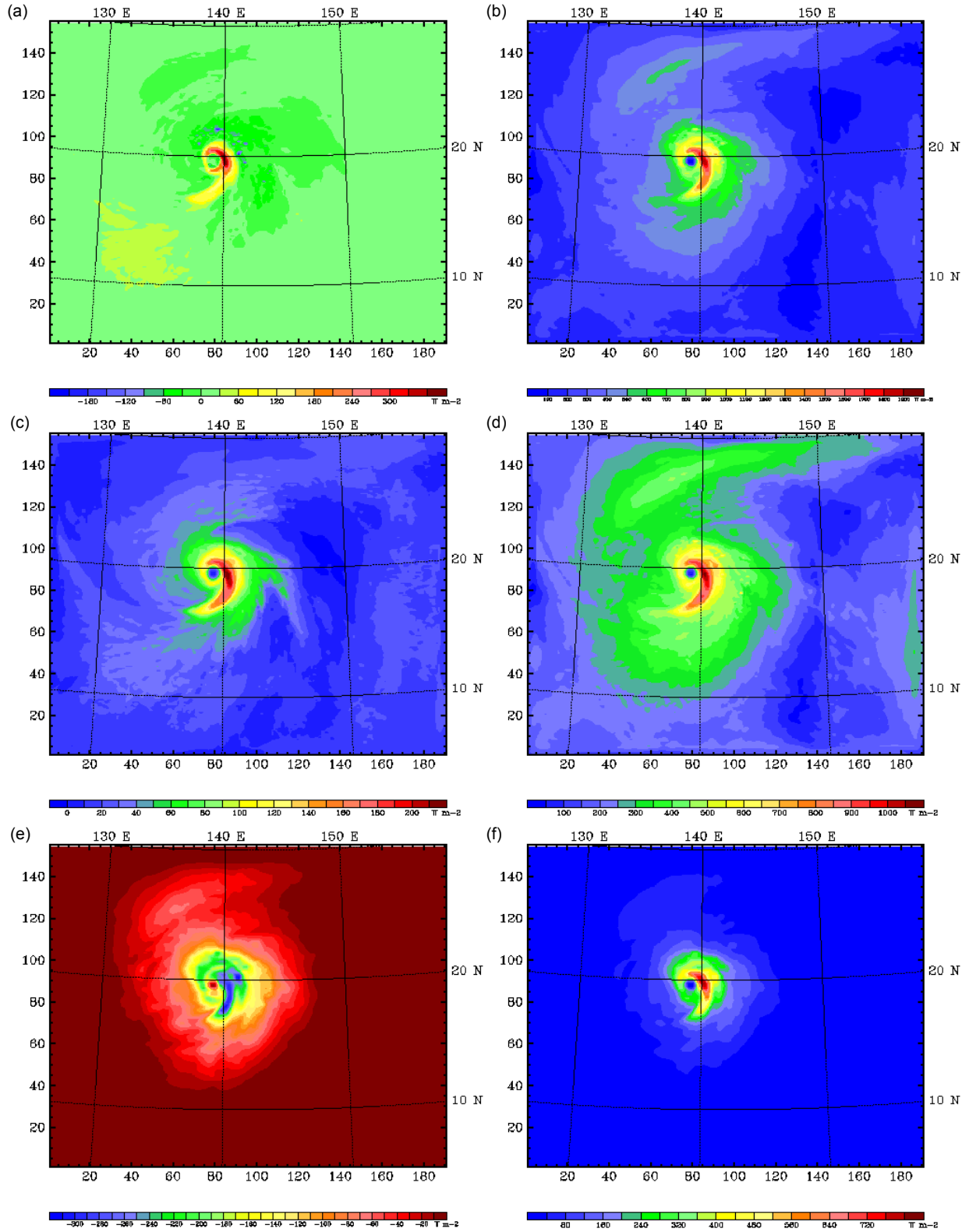
Figure 5. The simulated 48-h total sensible heat flux $H_{S,T}$ (a), total latent heat flux $H_{L,T}$ (b), direct sensible heat flux H_S (c), direct latent heat flux H_L (d), sea spray sensible heat flux $Q_{S,sp}$ (e), and sea spray latent heat flux $Q_{L,sp}$ (f), for experiment CPLFULL.